Shoreface Stratigraphy: Evolution and Morphology observations from southern Mozambique

By

Henna Lesley Draycott

215042441

Submitted in fulfilment of the academic requirements for the degree of

Master of Science in the

School of Agricultural, Earth and Environmental Science,

University of KwaZulu-Natal

Durban (Westville)

July 2024

As the candidate's supervisor I have approved this dissertation for submission.

Name: Professor Andrew N. Green Signed:[redacted]

COLLEGE OF AGRICULTURE, ENGINEERING AND SCIENCE

DECLARATION 1 - PLAGIARISM

I, HENNA L. DRAYCOTT, declare that:

1. The research reported in this thesis, except where otherwise indicated, is my original research.

2. This thesis has not been submitted for any degree or examination at any other university.

3. This thesis does not contain other persons' data, pictures, graphs or other information, unless specifically acknowledged as being sourced from other persons.

4. This thesis does not contain other persons' writing, unless specifically acknowledged as being sourced from other researchers. Where other written sources have been quoted, then:

a. Their words have been re-written but the general information attributed to them has been referenced

b. Where their exact words have been used, then their writing has been placed in italics and inside quotation marks, and referenced.

5. This thesis does not contain text, graphics or tables copied and pasted from the Internet, unless specifically acknowledged, and the source being detailed in the thesis and in the References sections.

Signed:

[redacted]

15/July/2024

COLLEGE OF AGRICULTURE, ENGINEERING AND SCIENCE

DECLARATION 2 - PUBLICATIONS

This dissertation is the product of research conducted by the first author (HL Draycott). The subsequent authors (Prof. AN Green, Prof. JAG Cooper; Loureiro, C) helped draft the manuscript as supervisor, data collectors and advisors. The basis of the research was conceptualised by the first author under close guidance from of the second author (Supervisor Prof. AN Green). The writing, preparation of the manuscripts and construction of figures are by the authors, unless otherwise stated. This thesis thus takes the form of a paper in the style and format of the journal *Marine Geology*.

Henna L. Draycott is affiliated with Geological Sciences, School of Agricultural, Earth and Environmental Sciences, University of KwaZulu-Natal.

Prof. Andrew Green and Andrew Cooper are affiliated with Geological Sciences, School of Agricultural, Earth and Environmental Sciences, University of KwaZulu-Natal and School of Environmental Sciences, University of Ulster, Coleraine BT52 1SA, UK.

Dr Carlos Loureiro is an assistant Professor affiliated with Geosciences, University of Algarve and Geological Sciences, School of Agricultural, Earth and Environmental Sciences, University of KwaZulu-Natal.

Draycott H. L, Green, A. N, Cooper, J. A. G., Loureiro, C. (in preparation). Shoreface Stratigraphy: Evolution and Morphology observations from southern Mozambique. *Marine Geology.*

Signed: [redacted]

Acknowledgements

Foremost, my gratitude to Professor Green for his supervision of this research. Not only has Professor Green been a supervisor, but my first inspiration to contribute to science in its true form, to improve today no matter what yesterday was like, and simply to be a real nice human being. It is a true honour to be your student and have your recognition of my abilities – this is something I will take with me through life. Thank you for your endless patience through the years, kindness, and for setting a fine example of Ubuntu.

It is an honour to thank Professor J.A.G Cooper and Dr C. Loureiro for their respective supervision and knowledge contribution to this research! Special thanks to Prof Cooper for his valuable feedback and input in the final drafting of this dissertation.

A special note to my family - Dad, my no.1 cheerleader, from whom I developed my curiosity for all things. Mum, from whom I have learned to direct and execute all that curiosity. My partner, who casts a spotlight on my strengths and served as a catalyst in the pursuit my goals. Finally, to my family that have carried me forward in life, I am endlessly grateful for the strong foundation that you provided me.

This research was made possible through funding from the NRF (National Research Foundation). Respective data collection was done by Professor Andrew Green and Bob De Decker.

Abstract

Shoreface morphology and stratigraphy are poorly documented but are acknowledged to be important influences on shoreline behaviour during changing sea level. A wide, low gradient wave-dominated shoreface off Xai-Xai in southern Mozambique is developed on the Holocene wave ravinement surface cut into deltaic sands punctuated by lithified aeolianite ridges. The 2 km-wide mobile shoreface sand body extends to -23 m depth and averages 10 m in thickness. Seismic stratigraphic analysis accompanied by seabed cores, reveals the shoreface to be underlain by a deltaic sedimentary sequence. The modern shoreface mimics the wave ravinement surface and this, in turn is influenced by the presence of aeolianite ridges that create a pronounced break in slope that defines the base of the modern shoreface. Comparison with theoretical shoreface profiles reveals contrasting interpretations depending upon the model chosen and emphasizes the acknowledged but still little understood role of geologic inheritance on shoreface morphology and evolution.

Table of Contents

Table of Figures:

1. Introduction

Understanding the evolution, morphology and multi-decadal behaviour of the shoreface remains a challenge because of a relative paucity of observations. Yet, because of its dynamic links to the surfzone and beach/dune environments, the shoreface is a major influence on future shoreline change during sea-level change. Further study of a range of shorefaces is required to enhance understanding of their evolution and role in coastal behaviour. Because morphological information on the shoreface is lacking, a theoretical shoreface profile is often created for use in shoreline evolution models (Swift, 1975; Daley and Cowell, 2012; Jaramillo et al., 2019). These profiles are described by some equation related chiefly to the mean grain size of the shoreface sediment (Dean 1991; Ortiz and Ashton, 2016). In predicting future shoreline behaviour, it is then usually assumed that this shoreface morphology is time-invariant and that it translates landward as sea level rises at the same rate as the beach and surf zone according to the “Bruun Rule” mechanism (Schwartz, 1967).

There are many objections to this approach including the observation that grain size cannot be definitively linked to profile slope (Pilkey et al., 1993), and that shorefaces often operate at different temporal scales to surf zones and beaches, giving rise to the potential for shoreface-surf zone decoupling during rapid sea level rise (Cooper et al., 2018). In addition, recent reviews have shown that active shorefaces exhibit wide variability in morphology (Hamon-Kerivel et al., 2020; Anthony and Aagaard, 2020). The reasons for these variations are not well understood, but Hamon-Kerivel et al. (2020) point out the role of underlying geology in creating accommodation space for shorefaces to exist. They also posit a link between sediment supply and shoreface morphology, with concavity associated with sediment scarcity, and convexity and associated shoreface-connected ridges reflecting increasing degrees of sediment abundance. Fire Island remains one of the few well-documented shorefaces and its temporal evolution and dynamics as expressed in shoreline-shoreface sediment exchanges have been documented (Schwab et al., 2013). These in part relate to the underlying geological framework (Hapke et al., 2010).

The aim in this paper is to document the morphology and stratigraphy of the shoreface of a little-known part of the SE African coast and to interpret its development in the context of underlying geological influences (subsurface lithology and morphology), sea-level change and long-term sediment supply. Is the geology and stratigraphy of this location like other contemporary regions of similar morphology in terms of regional geology and oceanography? Will long held models used in any shoreface setting be applicable to the nature of the morphology in this setting? In pursuing this investigation, we explore the currently poorly documented role of these factors on shoreface morphology and behaviour.

2. Literature Review

2.1 Shoreface stratigraphy in relation to southern Mozambique

The integration of different data sets (ground truthing seismic data in the form of well data, and conversely the use of seismic imaging to differentiate depositional settings that share log motifs) is integral to an effective and reliable interpretation of stratigraphy (Catuneanu, 2022). Seismic stratigraphy and seismic facies can be critical to interpreting underlying geology as well as mapping out geological history and sequence stratigraphy with the aspect of the third dimension. In 1977, Mitchum reported that seismic facies are distinguished by their seismic nature and the reflections they comprise, by means of a combination of reflection configuration, reflection continuity, reflection amplitude, reflection frequency or interval velocity. The description of individual packages of seismic reflections (seismic facies) are defined by reflector surfaces that enclose these packages with a different acoustic reflection pattern which is indicative of a bounding unconformity (Veeken and van Moerkerken, 2013). The internal reflection patterns, which are indicative of the depositional environment and relate to the distribution of the associated lithofacies, can be described accordingly as prograding, divergent, chaotic, parallel, subparallel and reflection free (Veeken and Moerkerken, 2013).

Catuneanu (2006) details the types of terminations that can be interpreted in seismic data as stratal terminations such as erosional truncations, onlaps, downlaps, toplaps and offlaps whereby the upper boundaries display erosional truncations, and the lower boundaries display onlap or downlap patterns in seismic section (Mitchum, 1977). By way of interpreting specific identifiers of stratal terminations, the type of syn-depositional shoreline shifts (progradation, aggradation, retrogradation) and evolution can be determined (Catuneanu, 2006).

Through wave action, the shoreface is a common source of long-term sediment supply to beaches (Cowell et al 2003; Kinsela et al., 2016) which can allow for the maintenance and even progradation of the shoreline where sea-level rise is slow and less than the rate of sediment supply (Fruergaard et al., 2018; Kinsela et al., 2020). Geologically, the shoreface environment is typically a depositional sandy wedge which grades seaward to silt, and grades landward to coarser sands and gravels respectively (Pemberton et al., 2012). Stratigraphically, a progradational succession of the shoreface would reflect offshore to foreshore related facies in an upward coarsening motif, punctuated by flooding surfaces related to small shifts in sea-level rise or sediment supply.

The subcontinent of Africa is dominated (~80%) by sandy shorelines from the coast of Mozambique, through South Africa, to Namibia (Cooper and Green, 2023). In the case of the southern

Mozambique coastal shelf, which is on the whole a sandy, wave dominated coastline (Cooper and Green, 2023), at the local scale there can be substantial variability in form and setting (Cooper et al., 2020). Along the SE African coastline, aeolianites and beachrocks in the shoreface stratigraphy and which crop out along the seafloor are commonplace (Flemming, 1981; Cooper and Green, 2016; De Lecea et al., 2016; Green et al., 2018).

It has widely and rigorously been discussed (i.e., Cooper et al., 2020; Wenau et al., 2020; Dyer et al., 2021) that there is more than one single response of coastal regions to sea level rise. And yet, it is still dictated by models that take into consideration specific responses to sea-level rise in isolation. Dyer et al., (2021) considered three options that have been used for modelling of shorelines in the response to sea-level rise:

1. The shoreline moves as a whole and there is complete reworking of shoreface deposits, leaving no remnants of the original shoreline (Swift and Moslow, 1982; Leatherman et al., 1983).
2. The shoreline migrates up the depositional profile and the initial shoreline is completely eradicated through erosional effects of the beachface (Bruun, 1962; Schwartz, 1967).
3. Overstepping of the shoreline due to rapid transgression leaves coastal landforms to be drowned and new ones form up-dip, thus preserving the original shoreline (Forbes et al., 1991; Swift et al., 1991).

Seismic data in the coastal marine environment along the southern Mozambique coastline have reported several distinctive shoreline features in the stratigraphy of the continental shelf related to various sea level cycles. Their presence lends themselves to overstepping, whereby transgression has resulted in the preservation of shorelines, topographic ridges and palaeo-coastlines (aeolianite ridges and beachrock) due to drowning and subsequent burial from the high sediment influx along this coastline (Green et al., 2014; Wenau et al., 2020).

2.2. Shoreface modelling

Shoreface modelling is important to forecast the effects of sea-level rise on coastal areas to aid human adaptation (Cooper and Green, 2023), as well as to best prepare current and future development plans in light of coastal risk. Reports on mechanisms that influence the shoreface, and thus, the shoreline, have been dominantly centred around using the classifications, mechanisms, and rates of wave-driven sediment supply, without paying much attention to various other factors, notably geological control (Pilkey et al., 1993), especially along sandy coasts.

It is generally accepted that coastal depositional systems follow the basic principles of shoreline retreat in response to sea-level rise (Swift et al., 1991), if the rate of sea-level rise exceeds the rate of sediment supply. Through wave action, the shoreface is a common source of long-term sediment supply to beaches in some areas (Cowell et al 2003; Kinsela et al., 2016) and this can allow for the maintenance or progradation of the shoreline where sea-level rise is slow and less than the rate of sediment supply (Fruergaard et al., 2018; Kinsela et al., 2020).

It has long been assumed by engineering practices that these two systems (upper and lower shoreface) are coupled to the beach, occur in equilibrium, and maintain profile equilibrium in response to change. Pilkey et al (1993) describe the example of a beach replenishment project where decisions (made on factors such as: grain size, type of fill material, amount of fill material and placement of fill on the profile) are dependent on data retrieved from models that create projected profiles of the shoreface. These are based on the assumption that the shoreface region reaches equilibrium, where the shape of the profile does not change in response to factors such as sea-level rise. However, other factors are often ignored (i.e., antecedent geological controls and accommodation space relative to the rate of sedimentation).

These equilibrium concepts are built on the Bruun Rule, whereby, Bruun's theory (Bruun, 1962) hypothesises that following sea-level rise, shore erosion is predictable. Subsequently a number of models created to predict shoreface trajectory are based on the equilibrium beach concept of the Bruun Rule such as the GENESIS model of Hanson and Kraus (1989); SBEACH (Larson and Kraus, 1989), Dean Model (Dean, 1991) and Ortiz and Ashton's (2016) approach.

The Bruun Rule (1962) is possibly the most straight forward concept used for shoreface trajectory in response to sea-level rise by using geometric rules to translate the shoreline. It presumes a steady shape shoreface slope whereby the whole shoreface profile is postulated to respond to sea-level rise due to mass conservation, thus, the shoreline retreats as a consequence (Ortiz and Ashton, 2016). Dean (1991) found that when wave energy is constant, the shoreface takes the form of a concave up morphological profile by conservatively adjusting to coastal erosion by shedding material from the upper shoreface and beach to the lower shoreface as sea-level rises (the Bruun rule).

3. Regional setting

The study area is situated along the coast near Xai-Xai, on the innermost portions of the Limpopo continental shelf of southern Mozambique (Fig. 1). The area occurs within the Delagoa Bight, a ~ 400 km long WSW-ENE-oriented structural offset marked by a progressive northward widening of the continental shelf and seaward displacement of the shelf break (Dyer et al., 2021). The shelf is narrowest in the south (< 15 km) and widens seawards to Ponta Zavora where it once again narrows with a more ESE-WNW coastal orientation (Fig. 1). The shelf is characterised by a thick succession of mid Pleistocene-age deposits (Wenau et al., 2020), mantled by late Pleistocene to Holocene deltaic and aeolian sequences (Dyer et al., 2021) (Fig. 2). Seismic reflection and multibeam bathymetric data from the mid to inner shelf regions reveal thick pro-delta muddy deposits which abut laterally extensive coast-parallel aeolianites to seaward (Dyer et al., 2021).

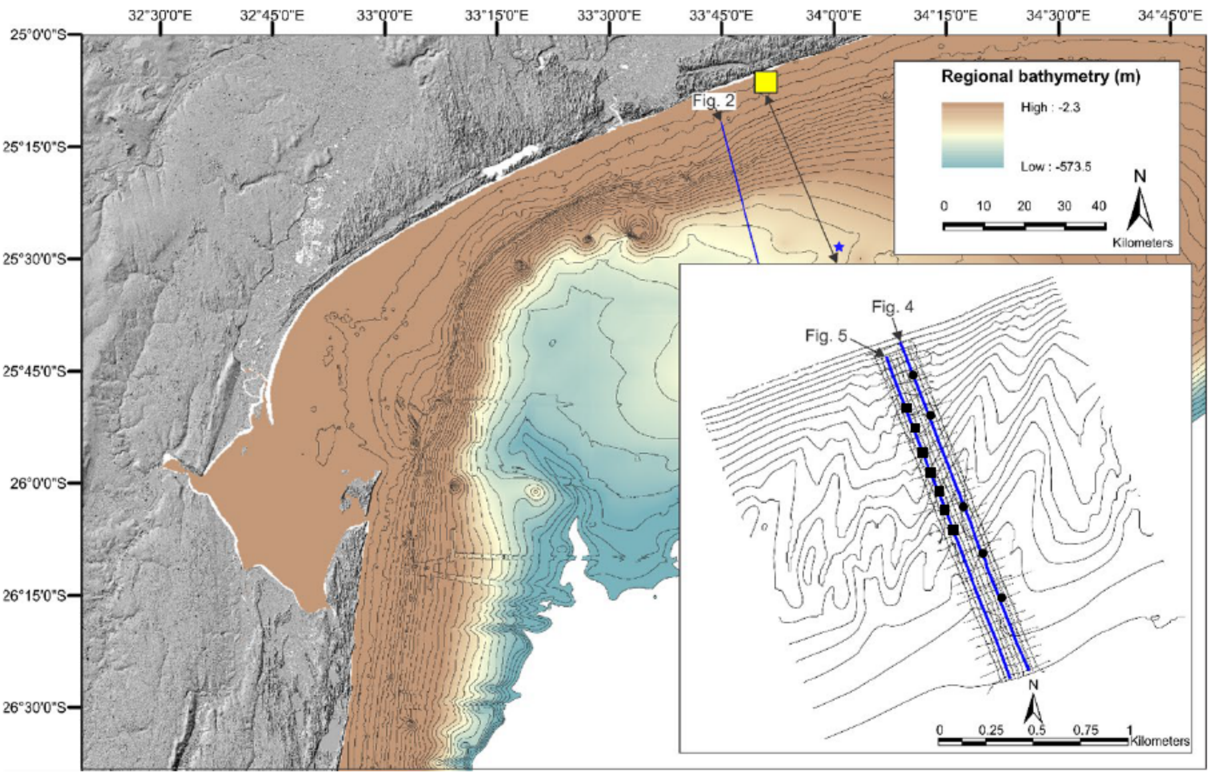

Figure 1. Locality map of Delagoa Bight area depicting the study area just off the coast of Xai-Xai, Mozambique (Moz). Blue lines = seismic profiles; Grey lines = tracklines of all the seismic profiles; Black dots = borehole locations; Black squares: = Jet probe localities; Blue star = ERA5 grid node. Bathymetry contours of the main map deepen seaward in 20-meter step intervals. Inset map portrays bathymetry contours with an interval of 1 meter.

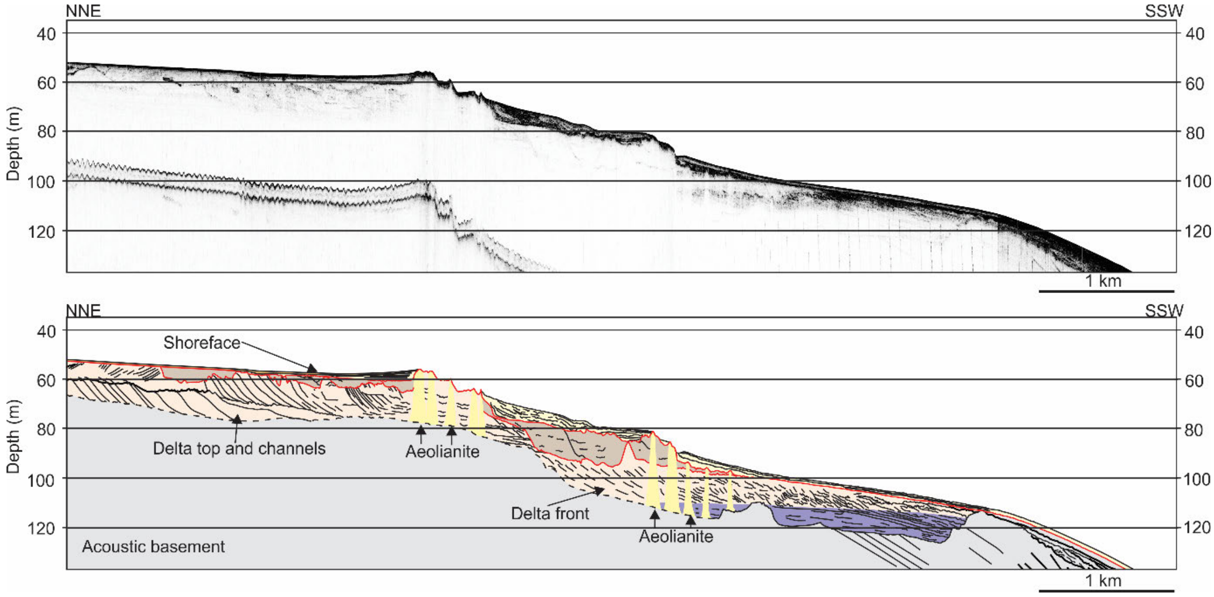

Figure 2. Seismic reflection profile from the mid shelf, immediately adjacent to the study area. (Adapted from Dyer et al., 2021). Note the prominent aeolianite with a basal depth of ~ 60 m, and the channelled delta-top and muddy prodelta facies that onlap the aeolianite ridge along its landward edge.

The adjoining coastal plain comprises Neogene to Holocene age coast-parallel linear dunes (Armitage et al., 2006; Botha and Porat, 2008), with active transgressive dune systems along its seaward-most margin (Miguel et al., 2018; 2019). These mantle and abut raised aeolianites and beachrocks along the coastline (Miguel et al., 2019). Isolated coastal waterbodies exist sporadically north of the Limpopo River and represent impoundment of the water table behind the main coastal barrier system (Miguel et al., 2019).

The southern Mozambican coastline is considered a high energy setting with average deep water wave heights of 1.5 m (Cooper and Pilkey, 2002) and with a mesotidal spring tidal range of 3 m (Sete et al., 2002). Hoguane et al. (1999) stated that the magnification of the tides along the Mozambican coast can be attributed to the shelf morphology as well as the influence of waves entering the Mozambique Channel from the south. The coast is dominated by a south-easterly swell regime and a northeast subordinate swell regime causing dominant longshore transport to the north (Hoguane et al., 1999; Preu et al., 2011).

The study area is oceanographically characterised by the Delagoa Bight Eddy (Fig. 1), a lee-eddy, formed by the southerly flowing Mozambique Current (Lutjeharms, 2006). In the littoral zone, this eddy forms a counterclockwise flow, that causes fluvial discharges from the Limpopo and subordinate rivers to flow north-eastward (Preu et al., 2011; Schüürman et al., 2019). The contemporary sedimentation on the continental shelf is thus mostly controlled by this north easterly current that is reported to flow at velocities of 25-30 cm s^{-2} up to 150 m depth (Lamont et al., 2010; Preu et al., 2011).

Fluvial discharge is the dominant source of terrigenous sediment input to the area (Flemming, 1981), with most of the sediment received from the Limpopo River (Meade, 1983). The smaller Lusuftu, Matola, and Inkomati Rivers also provide significant terrigenous materials to the area (Schüürman et al., 2019). Dyer et al. (2021) revealed ~20 m of deltaic sediments that have accumulated behind an aeolianite barrier on the mid to inner shelf directly offshore Xai-Xai. The large amount of fluvial-derived sediment to the shelf, the overall northward-directed transport regimes (Chemane at al., 1997), and the relatively energetic wave regime predispose the area's shoreface to thick accumulations of sediment that should be likely to overprint any geological control on shoreface morphology (Hamon-Kerivel et al., 2020, Anthony and Aagard, 2020).

4. Methodology

A 4 km^2 section of the upper and lower shoreface was mapped using a combination of geophysical techniques from depths of 2 to 25 m. Single-channel seismic reflection data were collected using two separate systems. A lower resolution 200J boomer system was employed to image the bedrock sediment interface in the shoreface. The data were collected using an Octopus 360 acquisition system coupled to an 18-element hydrophone array and resolve to ~ 0.7 m in the vertical domain. The boomer data were co-acquired with higher resolution 3.5 kHz pinger seismic reflection data using a grouping of 4 Massa transducers and recorded on a separate channel with the Octopus 360 system. These data were collected to image the internal architecture of the unconsolidated sediment wedge up to 2 m water depth (~ 20 cm resolution). The data were processed using the Hypack SBP utility where both boomer and pinger data were bottom tracked, bandpass and swell filtered. Streamer layback corrections were applied to all boomer data, in addition to GPS antennae offsets. All reflector picking was done in Hypack and referenced to a co-acquired bathymetry surface.

Multibeam bathymetry was collected using a 234 kHz RTS2000 system interfaced with a SUBSEA OCTANS motion reference unit. Positioning for all geophysical data was achieved using a DGPS of < 1 m accuracy. Sound velocity variations were modelled using several sound velocity probe casts. Tidal variations in the data were modelled based on a moored Aanderaa WLR7 tide gauge. All data plot to mean sea level and resolve to ~ 1 m and 0.1 m in the horizontal and vertical domains respectively.

To investigate the lithostratigraphy of the area, five continuous drill cores were retrieved by using a diamond drill and jack up barge. Each core was approximately 45 m long, and all were drilled along the seismic reflection section of interest in a coast-perpendicular fashion (Fig. 1). Cores were split and the material subject to grain size analyses using standard sieving techniques. In addition, water jet probes were deployed parallel to the drill cores and main seismic line of interest. The water jet probes ranged in length from 13 m to 19 m. The purpose of the drill cores and jet probes was to assess any down dip variability in shoreface composition.

To explore the morphodynamics of the shoreface in the study area, an equilibrium profile modelling approach was used to determine the shoreface morphodynamic state as proposed by Kinsela et al. (2020). This relied on the application of two complementary shoreface equilibrium profile models to determine if the contemporary shoreface is in graded equilibrium, in overfit or underfit disequilibrium according to the definitions of Daley and Cowell (2013).

Following Kinsela et al. (2020), the equilibrium profile model of Dean (1991, hereafter DN91), based on uniform energy dissipation, and the model proposed by Ortiz and Ashton (2016, hereafter OA16), based on the balance of sediment transport following Bowen (1980), were used to determine the theoretical equilibrium shoreface profile for the Xai-Xai coast, and compare it with the average shoreface profile determined from the multibeam bathymetry as well as the standard deviation, as best represents the variability around the mean profile.

By using the approach of Ortiz and Ashton (2016), the characteristic morphodynamic wave height and period for Chongoene was determined by weighting the wave height and period distribution and examining their contribution to sediment transport. The mean grain size and the +/- 1 standard deviation of the grain sizes were calculated for the surface sediments in the Chongoene shoreface. The sediment fall velocity was calculated using Soulsby's (1997) empirical equation to obtain a mean equilibrium profile as well as the expected range as is based on the standard deviation.

As proposed by Kinsela et al. (2020), the equilibrium profile was translated to the start of the lower shoreface, matching well with the start of the bathymetric profile. This is justified by the fact that seaward of this area is the surfzone and sediment transport processes which prove unsuitable for the Ortiz and Ashton (2016) model.

The application of DN91 equilibrium shoreface profile model the same sediment fall velocities for mean and +/- 1 standard deviation of the grain size were used. Offshore significant wave and peak wave period data from the nearest grid node (Fig. 1) of the ERA5 global reanalysis (Hersbach et al., 2020) were used, as ERA5 was found to appropriately represent mean wave conditions in the SW Indian Ocean coast, despite minor overestimation (underestimation) of wave height (period) (Fanti et al., 2023). Deepwater (~280 m water depth) ERA5 wave data were extracted for the period 1979-2021, and then shoaled to 30 m water depth using linear wave theory to obtain a more accurate representation of wave conditions along the shoreface of the study area.

5. Results

5.1. Seafloor morphology

The seafloor of the inner shelf is dominated by a series of high-relief shoreface-connected ridges (SCRs) (Figs. 1 and 3a). The ridge crests slope seaward at ≤ 0.5-1° (Fig. 3b) and extend seaward from the shoreline for approximately 1 km (Fig. 3a). Their crests are aligned coast-obliquely (NNE-SSW) (Fig. 1) and are spaced 400 m to 600 m apart. The ridge heights are between 3-4 m, and they are asymmetrical, with a 1.5°-2° slope on the western-facing slopes and gentler gradients on the eastern-facing slopes (Fig. 3b).

For the first ~1 km from the shoreline, the shoreface reflects a steep, linear to concave up profile between -5 m and -20 m (Fig. 3a). An elevation in the seabed occurs at -22 m and is associated with an abrupt change in seabed slope (Fig. 3b). In the lower part of the shoreface, seaward of the SCRs, and below 22 m depth, the seabed flattens, with a gentler (0° - 1°) gradient (Fig. 3b).

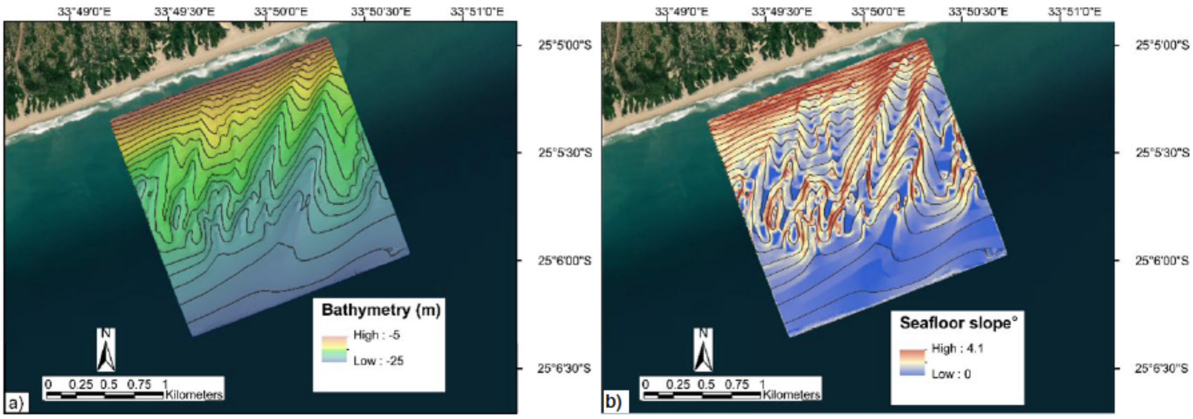

Figure 3. (a) Bathymetry demonstrating the morphology of several shoreface connected ridges terminating in ~ 25 m water depths. (b) Seafloor gradient, depicting the variability in slope and relief of the bathymetry. Coast-oblique shoreface connected ridges form ridge crests with lee faces that dip at up to 2° to the west, with asymmetrical flanks. Bathymetry contours have 1 meter interval.

5.2 Seismic and lithostratigraphy of the shoreface and underlying units

Several sedimentary units were identified based on seismic reflection profiles, drill cores and jet probe data (Fig. 1). Six main units are observed with five major seismic stratigraphic surfaces (Figs. 4 and 5). Figure 6 outlines the stratigraphic surfaces and unit thickness distribution of the shoreface and underlying substrate.

Unit 1

The lowermost unit is composed of indistinct, low to moderate amplitude seaward-dipping reflectors (Fig. 4a). Though reflectors are largely obscured by acoustic masking of the multiple, there is evidence in the boreholes of a seaward dipping pebbly gravel horizon (Surface 1) that marks the uppermost surface of the unit at depths of 48 m to 68 m below mean sea level (Fig. 4b). Surface 1 reflects an irregular relief horizon with minor NNE-SSW-oriented channels ~ 1 m deep and up to 70 m-wide in places (Fig. 6a).

Unit 2

High relief, acoustically opaque pinnacles with crest elevations from -50 m to -23 m overlie unit 1 (Figs. 4, 5 and 6b). These form several coast-parallel, 35 m-thick ridges comprising three main ridges with bases at between -55 m and -65 m (Fig. 6c). This unit characteristically obscures the acoustic signal and stratigraphy below (Figs. 4 and 5).

Units 3, 4 and 5

Unit 3 reflects a thick accumulation of sediment in the form of a seaward-pinching wedge (Figs. 4 and 5). The mostly sigmoidal-oblique internal reflectors dip seaward, with occasional landward-orientated reflectors. Their relationship with Surface 1 is not clear due to multiples masking the stratigraphy. Unit 3 is thickest to landward of Unit 2 where it reaches ~40 m in thickness (Fig. 6d). A narrow apron of Unit 3 ≤ 35 m thick abuts the seaward edge of the most landward ridge of Unit 2. Proximally, the unit comprises a fining upward package of medium to fine sands, with occasional shelly horizons occurring landward (Fig. 4a and Fig. 5).

Unit 4 comprises a series of moderate amplitude, tangential oblique prograding reflectors that downlap and onlap Surface 2 and which are in turn truncated by Surface 4, an irregular low to moderate amplitude reflector (Fig. 6e). The internal reflections transition into flat-lying parallel reflections to landward of the Unit 2 pinnacles. The lithological data from the boreholes reveal that this unit comprises a coarsening up sequence of medium to coarse sands, capped by a distinctive layer of pebbly gravel (Fig. 4a). This layer marks the presence of the irregular erosional surface (Surface 3) that separates unit 3 from the overlaying units 4 and 5.

Unit 5 comprises a series of tangential oblique, steeply dipping prograding reflections with minor internal discontinuities. The unit corresponds to a sandy, coarsening upward sediment body (Fig. 4a). This unit has a sudden change in structure of its reflectors from unit 4 and is thus represented as a different unit marked by the red line separating unit 4 and 5 in figure 4b. Unit 4 and 5 reach a combined thickness of ~ 22 m and cover the more inshore Unit 2 feature (Fig. 6f). The two units thicken considerably to landward of the deepest Unit 2 ridge. Both Units 4 and 5 are truncated by a gently seaward dipping, concave-up, high amplitude erosional reflector (Surface 4) (Fig. 6g). The surface is marked by the occurrences of shells and shell fragments and a slight increase in grain size from fine to coarse sand (Fig. 4a and Fig. 5).

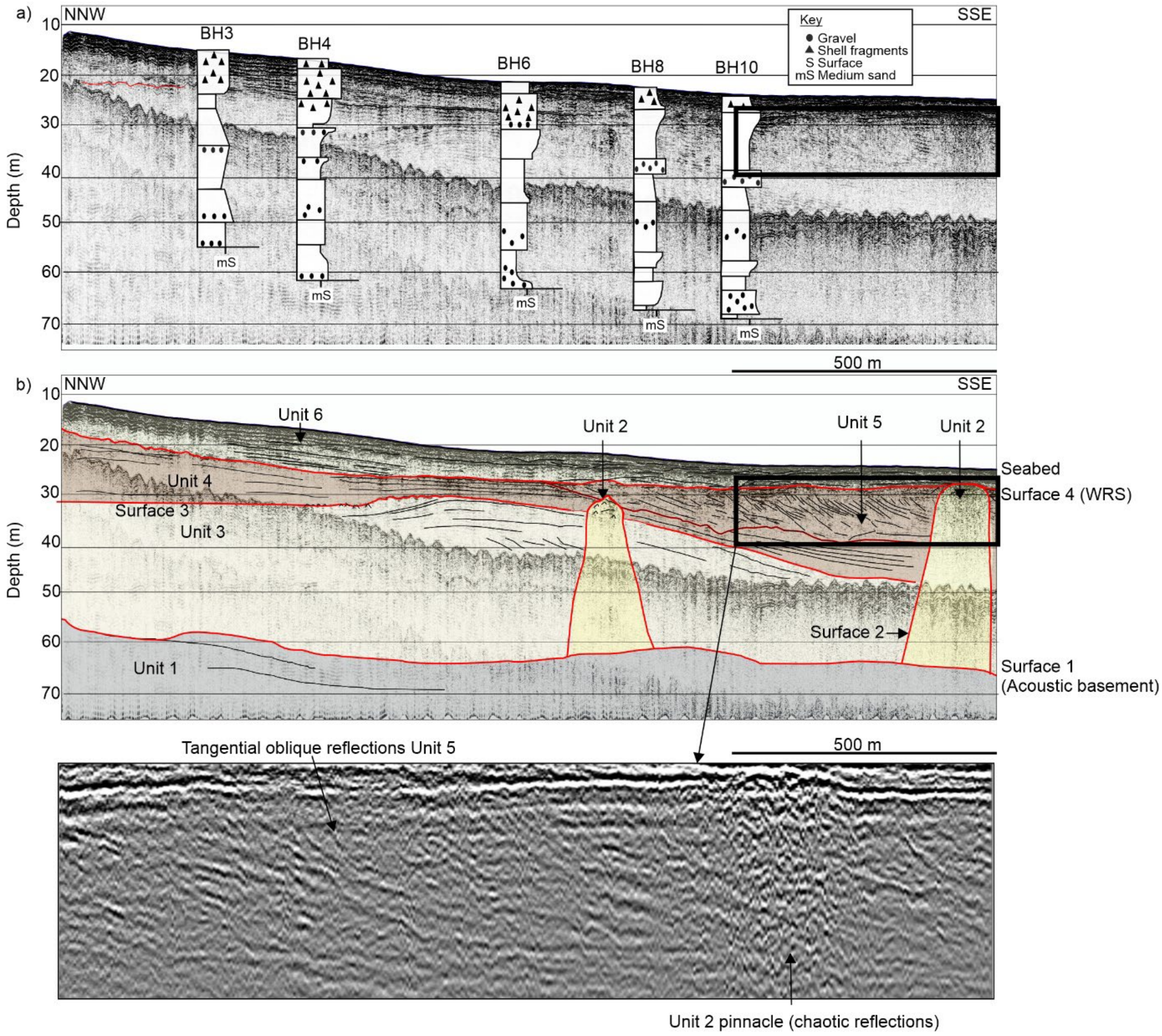

Figure 4. NNW-SSE trending boomer seismic reflection profile (For location see Fig. 1) with (a) boreholes overlain; (b) the main interpreted seismic stratigraphic units and key stratigraphic surfaces seismic stratigraphic surfaces in red - note the presence of two pinnacles of Unit 2.

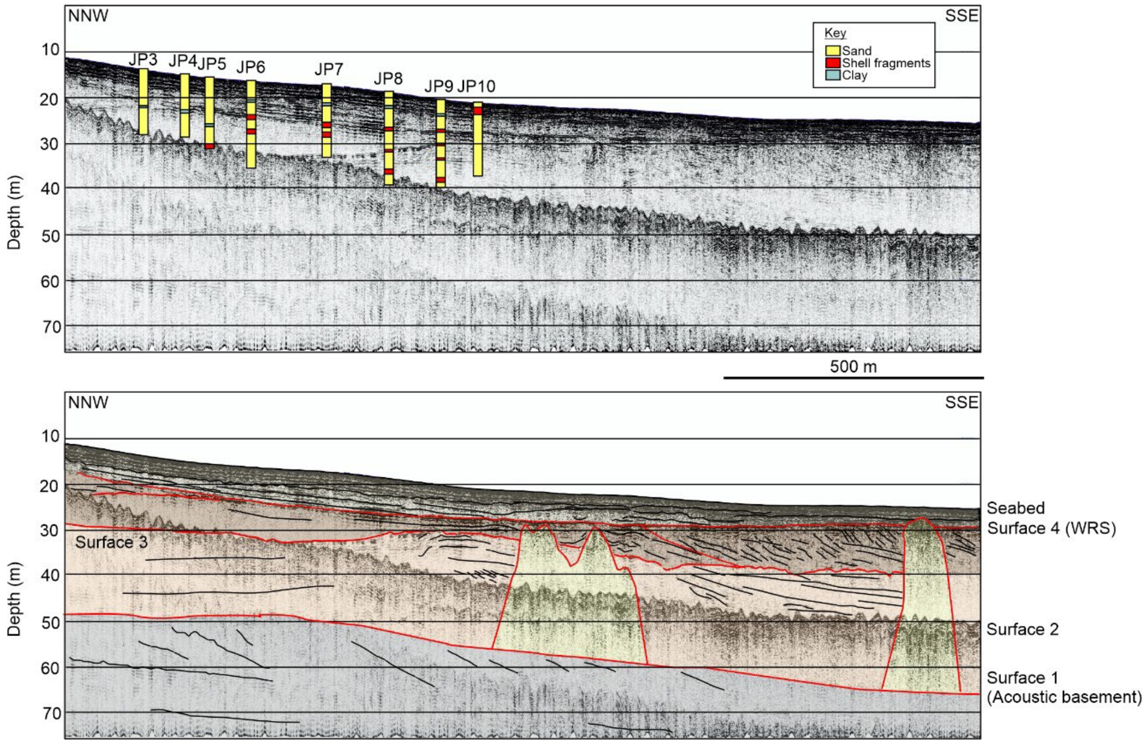

Figure 5. NNW-SSE trending boomer seismic reflection profile with the unit delineating surfaces. Jet probes (JP) are shown depicting the down dip change in sediment type.

Unit 6

Unit 6 is the youngest and shallowest unit, representative of the modern mobile shoreface. The unit comprises seaward dipping, planar to irregular, and sometimes wavy reflections with minor discontinuities evident to a depth of ~ 22 m. The unit appears to fine seawards with coarser sand and shell fragments associated with the more irregular shallow bathymetry to a depth of ~ 26 m (Fig. 4b), and finer materials occurring at the toe of the main seabed morphological features. Unit 6 thins seaward, with thicker accumulations of material (≤ 11 m) corresponding to the SCRs observed in the bathymetry (Fig. 3a).

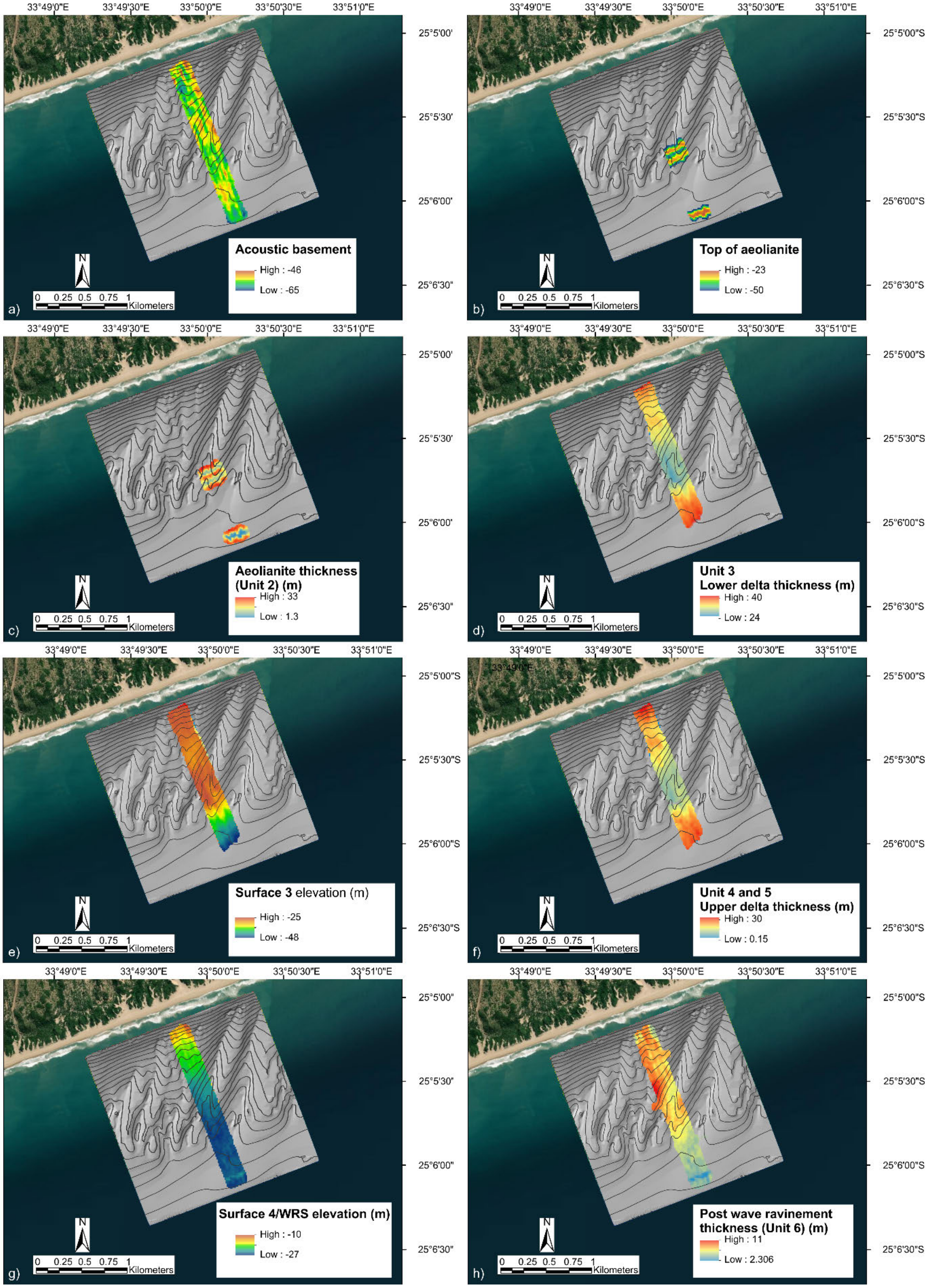

Figure 6. Depth/structure maps for the stratigraphy. (a) Elevation of acoustic basement, (b) top of aeolianite surface, (c) aeolianite thickness, (d) lower delta thickness, (e) surface 3 elevation, (f) upper delta thickness, (g) elevation of the wave ravinement, (h) post wave ravinement sediment thickness.

5.3. Internal architecture of major stratigraphic surfaces.

The acoustic basement (Surface 1, Fig. 4) is a low relief, gently seaward dipping unconformity that ranges in depth from -50 m to -67 m and on which Unit 2 rests (Fig. 4a). This gentle and uniform slope contrasts with the overlying seismic stratigraphic surfaces and contemporary bathymetry (Fig. 7a).

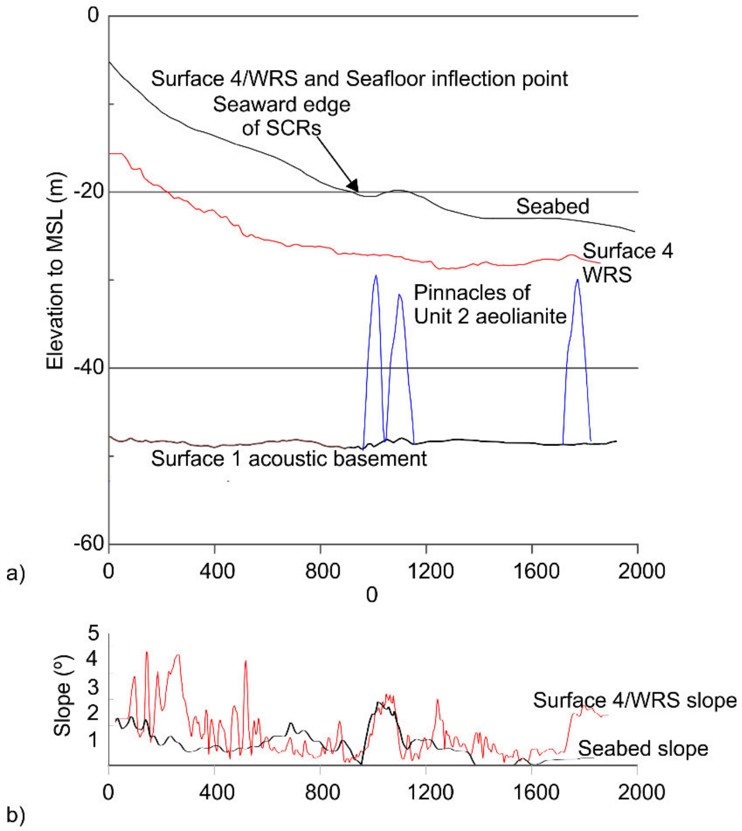

Figure 7. Cross sections of the major stratigraphic surfaces of the study area. a. Major stratigraphic surface elevations. There is a distinct similarity in the morphologies of surface 4 and the seabed. b . Cross sectional variation in slope of surface 4 (red) and the seabed (black). The inflection point in slope of both the seabed and Surface 4 corresponds with the pinnacles of the underlying unit 2.

The high relief pinnacles of Unit 2 dominate the stratigraphy and contribute to topographic variation in the key overlying stratigraphic surface 4 (Fig. 4a). Surface 4 has a pronounced increase in slope landward of the pinnacles of Unit 2 (Fig. 7b). This inflection point is in turn mirrored in the seabed bathymetry, where the bathymetric inflection point depicted in figure 7b accompanies the increase in the relief of Surface 4. Landward of these pinnacles, Surface 4 rises steeply from -30 m to -15 m, in a concave-up configuration (Fig. 7a), while seaward the gradient of Surface 4 flattens considerably, as does that of the seabed (Fig. 7b).

5.4. Modelled and measured shoreface profiles

The observed shoreface profile was compared to theoretically derived profiles for conditions in the study area. To determine the characteristic wave height and period, the wave conditions were weighted based on the contribution to sediment transport as proposed by OA16 and combined using a bivariate histogram (Fig. 8), with the centre of mass of the distribution corresponding to the morphodynamic wave height and period, calculated as 3.8 m and 12.1 seconds, respectively. To further investigate the influence of variable surface grain size on the theoretical shoreface profile, the OA16 model was also implemented considering the four main sand size classes identified in the cores (very fine, fine, medium, coarse).

Based on the weighted bivariate histogram of wave conditions on the coast at Xai-Xai (Fig. 8), the characteristic morphodynamic wave height and period used for modelling the equilibrium shoreface profile are 3.8 m and 12.1 s, respectively. These reveal effective wave conditions characteristic of a moderate to high-energy wave setting. Combined with grain size (mean = 364 mm, standard deviation 86 mm) and corresponding sediment fall velocity (mean = 0.047 m/s and standard deviation = 0.013 m/s) determined from borehole surface sedimentology, the theoretical equilibrium profiles indicate contrasting conditions (Fig. 9).

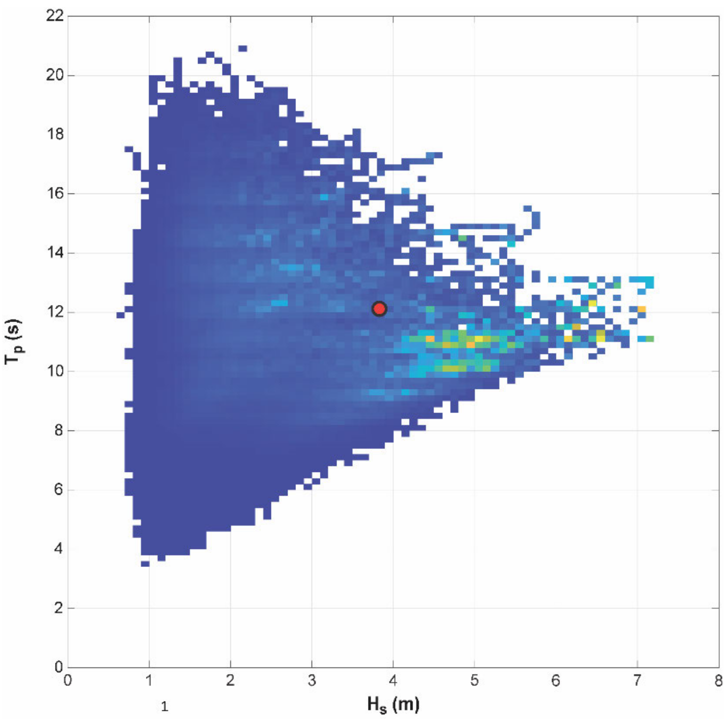

Figure 8. Weighted wave height and wave period distribution 2D histogram reflecting the characteristic morphodynamic wave height and the characteristic morphodynamic wave period for Xai-Xai (red dot).

Following Kinsela et al. (2020), equilibrium profiles determined using the OA16 model were translated to the origin of the surveyed profile seaward of the nearshore bars at -5 m water depth, as the model is based on wave shoaling processes and not appropriate to represent the general slope of the surf zone. Conversely, the DN91 equilibrium profile was not translated, and the origin is set at mean sea level, as this equilibrium profile model is considered to be representative of the surf zone and upper shoreface profile.

Both modelled equilibrium profiles evidence a concave up profile configuration that is similar to the shoreface bathymetry. According to DN91 the theoretical equilibrium profile is shallower than the observed bathymetric profile of the study area (Fig. 9a) and would be regarded as indicative of disequilibrium underfit in morphodynamic state. Based on the OA16 model, however, the theoretical equilibrium profile is deeper than the observed bathymetric profile, and the shoreface morphodynamic state suggests disequilibrium overfit (Fig. 9b). However, even considering the range of sediment size found in the seabed of the study site, represented by +/- 1 standard deviation of the mean grain size, both theoretical equilibrium profiles deviate significantly from the observed profile. As sediment size is often considered the primary control on shoreface equilibrium profile models, the OA16 model was also run for the same wave parameters but using the central value of sediments typical of sandy shorefaces (i.e., very fine sand, fine sand, medium sand, coarse sand). Improved agreement between observed and modelled shoreface equilibrium profile is achieved when the OA16 model is run for fine sand, with significant departures from the observed bathymetry in all other cases (Fig. 9c). Minor deviations between the observed and modelled profile for fine sand occur close to sections of higher bathymetric variability, represented by wider +/- 1 standard deviation bands around the mean observed profile (Fig. 9c).

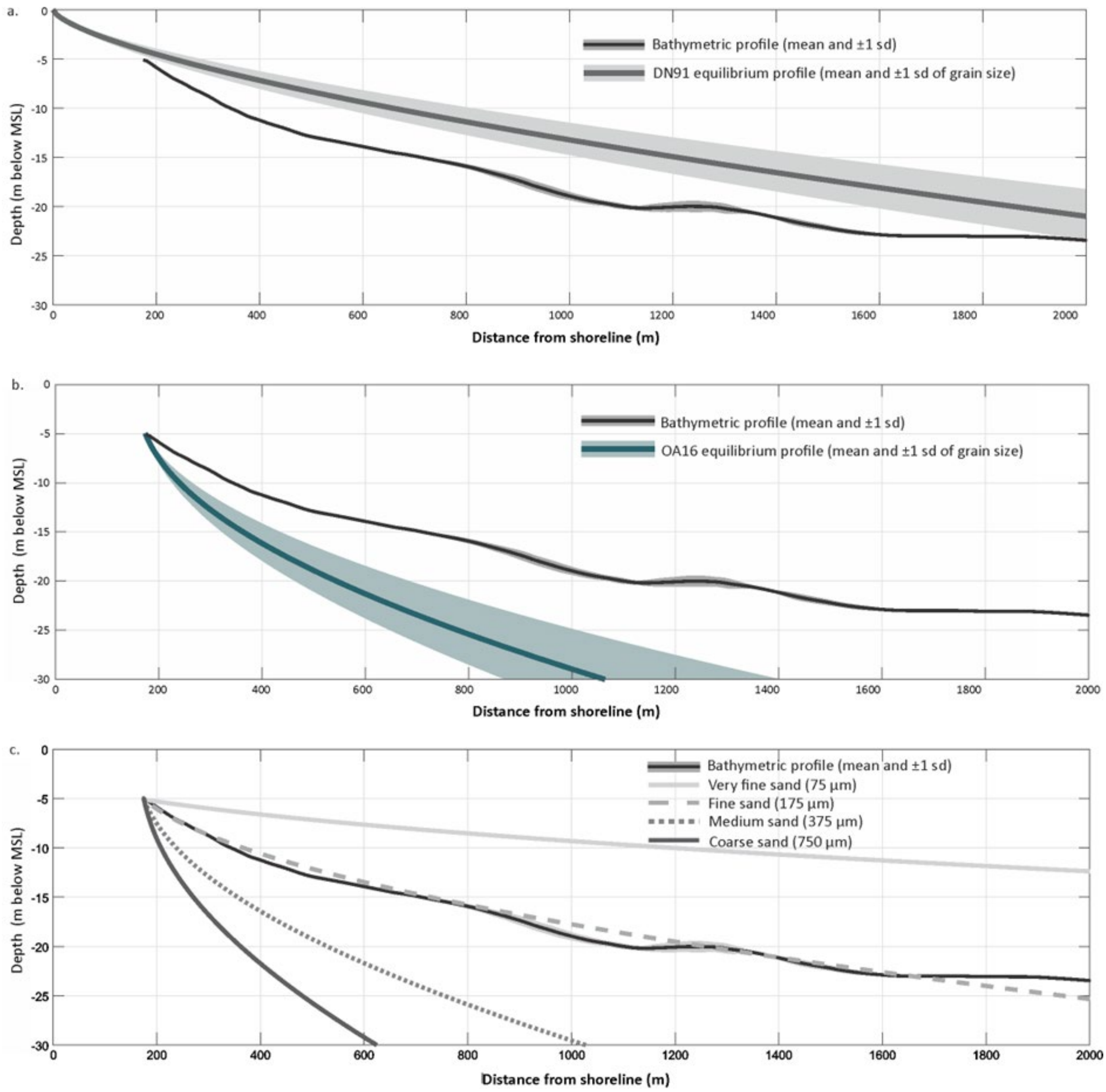

Figure 9. Shoreface depth profile of the Xai-Xai bathymetric profile run with the a. DN91 equilibrium profile. b. OA16 equilibrium profile using the mean surface grain size. c. Additional OA16 equilibrium profiles for the four main sand classes found in the surface sediments of the study area.

6. Discussion

6.1 Stratigraphic interpretation

Acoustic basement

Unit 1 is the oldest unit in the study area and constitutes the acoustic basement. Though the presence of gently seaward dipping reflections is visible, most of the unit is obscured by acoustic masking. This unit likely represents the landward continuation of the delta top deposits recognised by Dyer et al (2021). The age of deposition for the unit is uncertain. The seaward dipping pebbly gravel horizon of Surface 1 indicates a truncation of Unit 1 and likely relates to the erosional surface produced by migrating delta top channels during rising sea levels in the late Pleistocene and early Holocene (Dyer et al., 2021, Fig. 2).

Aeolianite pinnacles

The high relief and acoustically opaque nature of the pinnacles of Unit 2 are characteristic of aeolianite ridges observed throughout Maputo Bay (De Lecea et al., 2017), the Limpopo shelf (Wenau et al., 2020; Dyer et al., 2021) and the adjoining coastal plain (Miguel et al., 2019). Despite not being directly sampled in this study, samples of similar aeolianite from the KwaZulu-Natal shelf to the south of the study area reveal them to comprise well-sorted, carbonate-cemented sands (Richardson, 2005; Cawthra et al., 2018), the base of which may occur on unconsolidated sediment due to the variable position of the freshwater phreatic surface at the time of cementation (Bateman et al., 2004) and corresponds to the -75 m shoreline documented by Dyer et al (2021) seemingly forming at the onset of the Older Dryas event which closely followed meltwater pulse 1A. Once submerged, these form the most prominent topographic features of the SE African shelf (Green et al., 2014, Dyer et al., 2021).

Delta front deposits

The sigmoidal prograding reflectors of Unit 3, together with its mounded geometry and sporadically bi-directionally dipping reflections compares well with the internal geometry of other sandy deltaic bodies preserved in the shelf stratigraphy seaward of the study site (Dyer et al., 2021) and are likely associated with the Limpopo River. Similarly preserved features and with identical stratigraphic architectures were reported from sediment bodies on the adjacent South African shelf where the Thukela River also builds a subaqueous delta (Engelbrecht et al. 2020; 2022). Like those examples, the deposits of Unit 3 thicken where they abut aeolianite bodies to seaward, implying strong geological control on their development during the delta construction phase and later rollover phase.

The gently inclined flat-lying and uniformly parallel reflectors in the proximal part of Unit 4 transition to oblique tangential reflectors where Unit 2 is encountered. These are in turn overlain to seaward by another, package of oblique tangential reflections though without the same landward continuity into flat-lying reflections. Like Unit 3, these are interpreted as delta front deposits, with proximal delta top (flat-lying topsets) preserved in Unit 4, but separated from Unit 5 by the erosion that produced Surface 4.

The entire stack of Unit 3-5 thus represents periods of normal regressive sandy deltaic outbuilding, an interpretation corroborated by the upward-coarsening nature of the lithologies in the overall sediment package (Fig. 4 and 5). The position of the most landward aeolianite pinnacle dictated both the rollover of the Unit 4 delta, and the onlap point of the Unit 5 delta front with the previous Unit 4 delta body. The rollover positions are proximal relative to the modern shoreline, with rollover depths between 27 m to 30 m, indicating their deposition during lower than present sea levels during periods of high sediment supply. Unit 5's topsets are entirely truncated by Surface 4 and are linked to a second phase of delta construction (e.g. Dyer et al, 2021) whereby the delta is impounded by aeolianites around which there is overspilling.. Unit 5 prograding reflectors tie to this interpretation as it is evident from the peak of the seaward aeolianite ridge which is also where unit 5 separates from unit 4.

The erosional, high-amplitude Surface 4, revealed in the boreholes by an increased grain size associated with occurrences of shells and shell fragments, corresponds to the Holocene wave ravinement surface. Similar wave ravinement surfaces were documented by Pretorius et al. (2016; 2018) and De Lecea et al. (2017) on the SE African shelf. The overlying sediment is representative of a lower shoreface setting, marked by a seaward tapering wedge of sand that fines upward, indicative of progressive deepening of the shelf environment during landward shoreline migration (e.g., Zecchin, 20

Landward of the aeolianite pinnacles the wave ravinement surface profile evidences a consistent steepening, indicating a change in shoreline trajectory influenced by the presence of a harder substrate as the wave base translated over the mostly sand-dominated deltaic sediment bodies. In contrast, seaward of, and between the aeolianite pinnacles the ravinement profile is uniformly flat. The topsets of Unit 5 were removed by wave ravinement processes, however, the change in trajectory of the erosion surface marks the point where preservation of the underlying deltaic topsets of Unit 4 began.

Steepened trajectories of shoreface erosion can be ascribed to several factors. The primary factor is related to aggradation rates of the shoreface, whereby sediment supply determines the shoreline trajectory (Helland-Hansen and Martinsen, 1996). In such cases, an aggrading shoreface may define the ravinement trajectory by localised steepening and divergence of multiple erosion surfaces during the transgression process (Steel et al., 2000). Alternatively, the gradient over which the shoreline translates can control the accumulation of transgressive materials and in turn allow a divergence of the ravinement profile from the surface being transgressed (Cattaneo and Steel, 2003). Low-gradient settings produce thin shoreface deposits and a low angle ravinement profile that merges up-dip with the transgressed surface. In contrast, high gradient settings (assumed to be coupled to high sediment supply) may also produce steep ravinement profiles and multiple wave ravinement surfaces (Cattaneo and Steel, 2003).

In the case of the Xai-Xai shoreface, only one wave ravinement surface is observed capping the high-sediment-supply deltaic sequences. Though sediment supply has undeniably controlled to some extent the overall shoreface trajectory, the sudden steepening of the single wave ravinement profile, associated with the pinnacles of the underlying aeolianites is in contrast with the above models. Pretorius et al. (2016) and Engelbrecht et al. (2022) also recognised a situation where strong geological control by hard aeolianite substrate caused localised steepening of the wave ravinement and a decoupling of the shoreface from the surf zone, resulting in relict shoreface sediments preserved downdip in the offshore zone.

6.2 Sediment supply and geological control

Multiple phases of delta construction, with sediment accumulation of up to 40 m, indicates significant quantities of fluvial sediment input to the shelf, and a high degree of post-ravinement preservation of these materials.

An investigation of multiple sites along the U.S. coastline by Ortiz and Ashton (2016) found that modelled equilibrium shoreface profiles were comparatively similar to observed profiles for most locations, except where geological inheritance was strong. The results from that study supported the assertion of Dean (1991) that sediment grain size exerts the primary control on equilibrium shoreface slope in wave-dominated coastal settings. Comparing the equilibrium profiles computed for different grain sizes (Fig. 9c), under the characteristic wave energy conditions of Xai-Xai, only the fine sand modelled equilibrium profile matched the observed shoreface bathymetric profile. The measured grain size of the shoreface at Xai-Xai is of variable texture but does have a high proportion of material in the fine sand category.

In addition to the role of sediment texture and wave regime in determining the shoreface profile, the presence of underlying geological and stratigraphic features is also a fundamental control on shoreface morphology (Pilkey et al., 1993, Cooper and Pilkey, 2004, Cooper et al., 2018; Kirkpatrick and Green, 2018). Riggs et al.'s (1995) observations from a sediment-rich, wave-dominated transgressive shoreface in North Carolina include a finding on submarine headlands that bear comparison to the aeolianites in the study area. Riggs et al. (1995) showed that preservation of the headlands influenced the shoreface profile because they are manifest as bathymetric highs, cropping out in the mobile shoreface environment. Consequently, they influence incoming waves and currents and, in turn alter sediment dynamics and shoreface morphology. The crests of buried aeolianites, which intersect the wave ravinement surface, may also be an anchoring point for shoreface connected ridges.

6.3 Shoreface morphodynamic state

The morphodynamic state of sedimentary shorefaces can be considered according to the potential for sediment exchange and morphological change (Anthony and Aagaard, 2020), with potential implications for coupled shoreface and shoreline response to sea level rise (Kinsela et al., 2020). Based on the comparison between the theoretical shoreface equilibrium profile and the observed bathymetry, shoreface morphodynamic states can be classified as underfit or overfit disequilibrium or in graded equilibrium. (Daley and Cowel, 2012; Kinsela et al., 2020).

In the case of Xai-Xai, the DN91 and OA16 models indicate contrasting morphodynamic states, with disequilibrium underfit for DN91 (Fig. 10a), and disequilibrium overfit for OA16 (Fig. 10b). The absence of bathymetric information for the upper shoreface prevents an evaluation of the DN91 model in the surfzone, for which it is better suited. However, the results from Xai-Xai share similarities with sections of the New South Wales coast presented in Kinsela et al. (2020), where DN91 also evidences poor agreement indicative of underfit across most of the shoreface. Underfit disequilibrium is characterised by positive sediment accommodation, as the shoreface is too deep or too steep to reach equilibrium, allowing sediment mobilised in the upper shoreface to be transported offshore (Daley and Cowell, 2012). The abundant sediment supply and deltaic depositional setting associated with the Limpopo River, alongside the seaward dipping, planar to irregular reflectors of the thick modern mobile shoreface (Unit 6 – Fig 4 and 5), however, do not support such a conclusion for the Xai-Xai shoreface.

In contrast to DN91, the overfit disequilibrium predicted by the OA16 model (Fig. 10b) is indicative of a shallow shoreface with negative accommodation and overfilled with sediment, resulting in shoreward transport of sediment across the shoreface (Daley and Cowel, 2012). Support for this interpretation is provided by the abundant sediment supply previously discussed, but also by the controlling influence of the aeolianite pinnacles, which not only dammed delta front deposits in their lee but also influenced the wave ravinement trajectory and resultant surface profile, over which the modern sediment unit was deposited. These results for the Xai-Xai coast also suggest that the absence of physiographic features such as reefs or other rocky outcrops on the seabed, which are often invoked for poor agreement with shoreface equilibrium profiles (e.g. Thieler et al., 1995; Kinsela et al., 2020), disequilibrium can be caused by shallow subsurface geological features.

Overfit disequilibrium is associated with favourable conditions for onshore sediment transport from the lower shoreface, resulting in infilling of estuaries and generation of large sand dunes and ridges (Anthony and Aagaard, 2020). This is the case in along the Xai-Xai coast, with the near complete infilling of the Limpopo tidal basin and extensive dune systems along the coast. At present, the extent of shoreface overfit indicated by the OA16 modelled profile implies that excess sediment in the lower shoreface in Xai-Xai is far from being exhausted. For this coastal setting, it can then be assumed that the shoreface will continue to supply considerable amounts of sediment to the upper shoreface and beach, compensating the potential effects of rising sea levels and, consequently, maintaining shoreline stability or even accretion instead of retreat as postulated by approaches such as the Bruun rule.

7. Conclusions

The nearshore stratigraphy in the study area comprises 2 deltaic sequences overlying bedrock and separated by prominent aeolianite ridges. These units are truncated by the transgressive ravinement surface which shows a marked change in shore-normal gradient coincident with the underlying aeolianite pinnacles.

The transgressive ravinement surface is overlain by ca.10 m of shoreface sediment and the modern seabed slope largely mirrors that of the ravinement surface. The modern shoreface comprises mobile sandy sediment and is fronted by a sequence of SCRs that point to sediment abundance.

The shoreface is influenced by multiple dynamic and geological variables, but no single model has conceptualised the influence of geological inheritance on the shoreface in addition to sea-level rise. At Xai-Xai the comparison of predicted shoreface profiles to the measured situation produce enigmatic and opposing results. On the basis of the thick sediment volume and shoreface-connected ridges, a sediment-abundant 'overfit' interpretation is favoured. The shoreface underlying stratigraphy points to additional geological controls on the geometry and trajectory of the shoreface during and since the Holocene. In particular, submerged aeolianite ridges enhanced sediment retention/impoundment in the nearshore. Thus, ensuring the stability of shoreline position and preventing SLR-induced erosion.

8. References

1. Anthony, E.J. and Aagaard, T., 2020. The lower shoreface: Morphodynamics and sediment connectivity with the upper shoreface and beach. *Earth-Science Reviews*, *210*, p.103334.
2. Armitage, S.J., Botha, G.A. and Duller, G., 2006. The formation and evolution of the barrier islands of Inhaca and Bazaruto, Mozambique. *Geomorphology*, *82*, pp.295-308.
3. Bateman, M.D., Holmes, P.J., Carr, A.S., Horton, B.P. and Jaiswal, M.K., 2004. Aeolianite and barrier dune construction spanning the last two glacial–interglacial cycles from the southern Cape coast, South Africa. *Quaternary Science Reviews*, *23*(14-15), pp.1681-1698.
4. Bowen, A. J. (1980), Simple models of nearshore sedimentation; beach profiles and longshore bars. In S. B. McCann (Ed.), The Coastline of Canada, Geological Survey of Canada, Paper 80–10, 1–11.
5. Bruun, P., 1962. Sea-level rise as a cause of shore erosion. *Journal of the Waterways and Harbors Division*, *88*(1), pp.117-130.
6. Cattaneo, A. and Steel, R.J., 2003. Transgressive deposits: a review of their variability. *Earth-Science Reviews*, *62*(3-4), pp.187-228.
7. Catuneanu, O., 2022. *Principles of sequence stratigraphy*. Newnes.
8. Cawthra, H.C., Jacobs, Z., Compton, J.S., Fisher, E.C., Karkanas, P. and Marean, C.W., 2018. Depositional and sea-level history from MIS 6 (Termination II) to MIS 3 on the southern continental shelf of South Africa. *Quaternary Science Reviews*, *181*, pp.156-172.
9. Chemane, D., Motta, H. and Achimo, M., 1997. Vulnerability of coastal resources to climate changes in Mozambique: a call for integrated coastal zone management. *Ocean & Coastal Management*, *37*(1), pp.63-83.
10. Cooper, J.A.G., Pilkey, O.H., 2002. The Barrier Islands of Southern Mozambique. J. Coast. Res. Spec. Issue 36, 164–172. https://doi.org/10.2112/1551-5036-36. sp1.164.
11. Cooper, J.A.G. and Pilkey, O.H., 2004. Sea-level rise and shoreline retreat: time to abandon the Bruun Rule. *Global and Planetary Change*, *43*(3-4), pp.157-171.
12. Cooper, J.A.G. and Green, A.N., 2016. Geomorphology and preservation potential of coastal and submerged aeolianite: examples from KwaZulu-Natal, South Africa. *Geomorphology*, *271*, pp.1-12.
13. Cooper, J.A.G., Green, A.N. and Loureiro, C., 2018. Geological constraints on mesoscale coastal barrier behaviour. *Global and Planetary Change*, *168*, pp.15-34.
14. Cooper, J.A.G. and Green, A.N., 2023. Southern African sandy coasts in the context of near-future sea-level rise. *Transactions of the Royal Society of South Africa*, *78*(3), 149-166.

15. Cowell, P.J., Stive, M.J., Niedoroda, A.W., de Vriend, H.J., Swift, D.J., Kaminsky, G.M. and Capobianco, M., 2003. The coastal-tract (part 1): a conceptual approach to aggregated modeling of low-order coastal change. *Journal of Coastal Research*, pp.812-827.

16. Daley, M. and Cowell, P.J., 2012. Long-term shoreface response to disequilibrium-stress: a conundrum for climate change. In Proceedings of the 22nd NSW Coastal Conference, Port Macquarie. 16 p.

17. Dean, R.G., 1991. Equilibrium beach profiles: characteristics and applications. *Journal of Coastal Research*, pp.53-84.

18. De Lecea, A.M., Green, A.N., Strachan, K.L., Cooper, J.A.G. and Wiles, E.A., 2017. Stepped Holocene sea-level rise and its influence on sedimentation in a large marine embayment: Maputo Bay, Mozambique. *Estuarine, Coastal and Shelf Science*, *193*, pp.25-36.

19. Dingle, R.V., Goodlad, S.W. and Martin, A.K., 1978. Bathymetry and stratigraphy of the northern Natal Valley (SW Indian Ocean): a preliminary account. *Marine Geology*, *28*(1-2), pp.89-106.

20. Dyer, S.E., Green, A.N., Cooper, J.A.G., Hahn, A. and Zabel, M., 2021. Response of a wave-dominated coastline and delta to antecedent conditioning and fluctuating rates of postglacial sea-level rise. *Marine Geology*, *434*, p.106435.

21. Engelbrecht, L., Green, A.N., Cooper, J.A.G., Hahn, A., Zabel, M. and Mackay, C.F., 2020. Construction and evolution of submerged deltaic bodies on the high energy SE African coastline: The interplay between relative sea level and antecedent controls. *Marine Geology*, *424*, p.106170.

22. Engelbrecht, L.D., Green, A.N., Cooper, J.A.G. and Mackay, C.F., 2022. Antecedent geological control on transgressive delta and shoreline preservation: Examples from the SE African shelf. *Marine Geology*, *454*, p.106934.

23. Fanti, V., Ferreira, Ó., Kümmerer, V. and Loureiro, C., 2023. Improved estimates of extreme wave conditions in coastal areas from calibrated global reanalyses. *Communications Earth & Environment*, *4*(1), p.151. Flemming, B.W., 1981. Factors controlling shelf sediment dispersal along the southeast African continental margin. *Marine Geology*, *42*(1-4), pp.259-277.

24. Flemming, B.W., 1981. Factors controlling shelf sediment dispersal along the southeast African continental margin. *Marine Geology*, *42*(1-4), pp.259-277.

25. Forbes, D.L., Taylor, R.B., Orford, J.D., Carter, R.W.G. and Shaw, J., 1991. Gravel-barrier migration and overstepping. *Marine Geology*, *97*(3-4), pp.305-313.

26. Fruergaard, M., Johannessen, P.N., Nielsen, L.H., Nielsen, L., Møller, I., Andersen, T.J., Piasecki, S. and Pejrup, M., 2018. Sedimentary architecture and depositional controls of a Holocene wave-dominated barrier-island system. *Sedimentology*, *65*(4), pp.1170-1212.

27. Green, A.N., Cooper, J.A.G. and Salzmann, L., 2014. Geomorphic and stratigraphic signals of postglacial meltwater pulses on continental shelves. *Geology*, *42*(2), pp.151-154.

28. Green, A.N., Cooper, J.A.G., Wiles, E.A. and De Lecea, A.M., 2015. Seismic architecture, stratigraphy and evolution of a subtropical marine embayment: Maputo Bay, Mozambique. *Marine Geology*, *369*, pp.300-309.

29. Green, A.N., Cooper, J.A.G. and Salzmann, L., 2018. The role of shelf morphology and antecedent setting in the preservation of palaeo-shoreline (beachrock and aeolianite) sequences: the SE African shelf. *Geo-Marine Letters*, *38*, pp.5-18.

30. Hamon-Kerivel, K., Cooper, A., Jackson, D., Sedrati, M. and Pintado, E.G., 2020. Shoreface mesoscale morphodynamics: A review. *Earth-Science Reviews*, *209*, p.103330.

31. Hamon-Kerivel, K., Jackson, D.W., Guisado-Pintado, E., Cooper, A. and Sedrati, M., 2023. Spatial and temporal variability of shorefaces: A morpho-hydrodynamic controlled system. *Estuarine, Coastal and Shelf Science*, *281*, p.108162.

32. Hapke, Cheryl J., Erika E. Lentz, Paul T. Gayes, Clayton A. McCoy, Rachel Hehre, William C. Schwab, and S. Jeffress Williams. "A review of sediment budget imbalances along Fire Island, New York: can nearshore geologic framework and patterns of shoreline change explain the deficit?." *Journal of Coastal Research* 26, no. 3 (2010): 510-522.

33. Helland-Hansen, W. and Martinsen, O.J., 1996. Shoreline trajectories and sequences; description of variable depositional-dip scenarios. *Journal of Sedimentary Research*, *66*(4), pp.670-688.

34. Hersbach, H,. Bell, B,. Berrisford, P,. et al. The ERA5 global reanalysis. Q J R Meteorol Soc. 2020; 146: 1999– 2049.

35. Hoguane, A.M., Hill, A.E., Simpson, J.H. and Bowers, D.G., 1999. Diurnal and tidal variation of temperature and salinity in the Ponta Rasa mangrove swamp, Mozambique. *Estuarine, Coastal and Shelf Science*, *49*(2), pp.251-264.

36. Jaramillo, C., Jara, M.S., González, M. and Medina, R., 2020. A shoreline evolution model considering the temporal variability of the beach profile sediment volume (sediment gain/loss). *Coastal Engineering*, *156*, p.103612.

37. Kinsela, M.A., Daley, M.J. and Cowell, P.J., 2016. Origins of Holocene coastal strandplains in Southeast Australia: Shoreface sand supply driven by disequilibrium morphology. *Marine Geology*, *374*, pp.14-30.

38. Kinsela, M.A., Hanslow, D.J., Carvalho, R.C., Linklater, M., Ingleton, T.C., Morris, B.D., Allen, K.M., Sutherland, M.D. and Woodroffe, C.D., 2020. Mapping the Shoreface of Coastal

Sediment Compartments to Improve Shoreline Change Forecasts in New South Wales, Australia. *Estuaries and Coasts*.

39. Kirkpatrick, L.H. and Green, A.N., 2018. Antecedent geologic control on nearshore morphological development: The wave dominated, high sediment supply shoreface of southern Namibia. *Marine Geology*, *403*, pp.34-47.
40. Lamont, T., Roberts, M.J., Barlow, R.G., Morris, T. and van den Berg, M.A., 2010. Circulation patterns in the Delagoa Bight, Mozambique, and the influence of deep ocean eddies. *African Journal of Marine Science*, *32*(3), pp.553-562.
41. Leatherman, S.P., 1983. Barrier dynamics and landward migration with Holocene sea-level rise. *Nature*, *301*(5899), pp.415-417.
42. Lutjeharms, J.R., 2006. *The Agulhas current retroflection* (pp. 151-207). Springer Berlin Heidelberg.
43. Miguel, L.L.A.J. and Castro, J.W.A., 2018. Aeolian dynamics of transgressive dunefields on the southern Mozambique coast, Africa. *Earth Surface Processes and Landforms*, *43*(12), pp.2533-2546.
44. Miguel, L.L.A.J., Nehama, F.P.J. and Castro, J.W.A., 2019. Lagoon-barrier system response to recent climate conditions and sea level rise, Mozambique, Africa. *Estuarine, Coastal and Shelf Science*, *216*, pp.71-86.
45. Milliman, J.D. and Meade, R.H., 1983. World-wide delivery of river sediment to the oceans. *The Journal of Geology*, *91*(1), pp.1-21.
46. Mitchum Jr, R.M., Vail, P.R. and Thompson III, S., 1977. Seismic stratigraphy and global changes of sea level: Part 2. The depositional sequence as a basic unit for stratigraphic analysis: Section 2. Application of seismic reflection configuration to stratigraphic interpretation.
47.
48. Ortiz, A.C. and Ashton, A.D., 2016. Exploring shoreface dynamics and a mechanistic explanation for a morphodynamic depth of closure. *Journal of Geophysical Research: Earth Surface*, *121*(2), pp.442-464.
49. Pemberton, S.G., MacEachern, J.A., Dashtgard, S.E., Bann, K.L., Gingras, M.K. and Zonneveld, J.P., 2012. Shorefaces. In *Developments in Sedimentology* (Vol. 64, pp. 563-603). Elsevier.
50. Pilkey, O.H., Young, R.S., Rîggs, S.R., Smith, A.S., Wu, H. and Pilkey, W.D., 1993. The concept of shoreface profile of equilibrium: a critical review. *Journal of Coastal Research*, pp.255-278.
51. Porat, N. and Botha, G., 2008. The luminescence chronology of dune development on the Maputaland coastal plain, southeast Africa. *Quaternary Science Reviews*, *27*(9-10), pp.1024-1046.

52. Pretorius, L., Green, A. and Cooper, A., 2016. Submerged shoreline preservation and ravinement during rapid postglacial sea-level rise and subsequent "slowstand". *Bulletin*, *128*(7-8), pp.1059-1069.
53. Pretorius, L., Green, A.N. and Andrew Cooper, J., 2018. Submerged beachrock preservation in the context of wave ravinement. *Geo-Marine Letters*, *38*, pp.19-32.
54. Preu, B., Spieß, V., Schwenk, T. and Schneider, R., 2011. Evidence for current-controlled sedimentation along the southern Mozambique continental margin since Early Miocene times. *Geo-Marine Letters*, *31*, pp.427-435.
55. Riggs, S.R., Cleary, W.J. and Snyder, S.W., 1995. Influence of inherited geologic framework on barrier shoreface morphology and dynamics. *Marine Geology*, *126*(1-4), pp.213-234.
56. Schüürman, J., Hahn, A. and Zabel, M., 2019. In search of sediment deposits from the Limpopo (Delagoa Bight, southern Africa): Deciphering the catchment provenance of coastal sediments. *Sedimentary Geology*, *380*, pp.94-104.
57. Schwab, W.C., Baldwin, W.E., Hapke, C.J., Lentz, E.E., Gayes, P.T., Denny, J.F., List, J.H. and Warner, J.C., 2013. Geologic evidence for onshore sediment transport from the inner continental shelf: Fire Island, New York. *Journal of Coastal Research*, *29*(3), pp.526-544.
58. Schwartz, M.L., 1967. The Bruun theory of sea-level rise as a cause of shore erosion. *The Journal of Geology*, *75*(1), 76-92.
59. Sete, C.I., Ruby, J. and Dove, V., 2002. Seasonal variation of tides, currents, salinity and temperature along the coast of Mozambique.
60. Soulsby, R.L., 1997. Dynamics of marine sands: a manual for practical applications. *Oceanographic Literature Review*, *9*(44), p.947.
61. Steel, R.J., Crabaugh, J., Schellpeper, M., Mellere, D., Plink-Bjorklund, P., Deibert, J. and Loeseth, T., 2000. Deltas vs. rivers on the shelf edge: their relative contributions to the growth of shelf-margins and basin-floor fans (Barremian and Eocene, Spitsbergen).
62. Swift, D.J., 1975. Barrier-island genesis: evidence from the central Atlantic shelf, eastern USA. *Sedimentary Geology*, *14*(1), pp.1-43.
63. Thieler, E.R., Brill, A.L., Cleary, W.J., Hobbs III, C.H. and Gammisch, R.A., 1995. Geology of the Wrightsville Beach, North Carolina shoreface: Implications for the concept of shoreface profile of equilibrium. *Marine Geology*, *126*(1-4), pp.271-287.
64. Veeken, P. and Van Moerkerken, B., 2013. Seismic stratigraphic techniques. *Seismic stratigraphy and depositional facies models*, pp.105-214.
65. Wenau, S., Preu, B. and Spiess, V., 2020. Geological development of the Limpopo Shelf (southern Mozambique) during the last sea level cycle. *Geo-Marine Letters*, *40*, pp.363-377.

66. Zecchin, M., 2007. The architectural variability of small-scale cycles in shelf and ramp clastic systems: The controlling factors. *Earth-Science Reviews, 84(1-2),* pp.21-55.